A Self-Frequency Restoration Control Based on Droop Strategy for Autonomous Microgrid

Ronald Jackson*‡, Shamsul Aizam Zulkifli*‡, Noor Mazliza Badrul Sham*, Erum Pathan*

*Department of Electrical Power Engineering, Faculty of Electrical and Electronic Engineering,

Universiti Tun Hussein Onn Malaysia (UTHM), Malaysia

(ronaldjackson91@yahoo.com, aizam@uthm.edu.my, noormazliza@gmail.com, erumasad79@gmail.com)

‡Corresponding Author; Ronald Jackson, Shamsul Aizam Zulkifli, Department of Electrical Power Engineering, Faculty of Electrical and Electronic Engineering, Universiti Tun Hussein Onn Malaysia (UTHM), 86400 Parit Raja, Batu Pahat, Johor, Malaysia, Tel: +6074537559, Fax: +6074538387, ronaldjackson91@yahoo.com, aizam@uthm.edu.my

Received: 05.03.2019 Accepted: 22.03.2019

Abstract- This paper presents a frequency self-restoration by minimizing the frequency transient time response when applied to an autonomous microgrid configuration. At the same time, it also offers a good power-sharing among the distributed generations (DGs) when the load-rated power is changed but maintains the DGs' power supplies. This self-frequency restoration control is different from the conventional droop in that it includes the frequency limitation condition in order to have a fast frequency restoration during load changes and to ensure an accurate active and reactive power sharing. The proposed controller is tested in parallel DGs configuration and associated with different power load ratings during off-grid condition. The simulation study shows the effectiveness of the proposed controller when the DG units are in plug-in/out and under load circumstances for an autonomous microgrid condition. The simulation results exhibit improved performance and robustness for the proposed control method in recovering the frequency in a very short of time and in controlling the allowable active and reactive powers according to the requested power from the loads.

Keywords: Droop control, microgrid, distributed generations, frequency restoration.

1. Introduction

In the modern era, the renewable energy sector is becoming more interesting to be explored due to its demand and high penetration into the integrated microgrid system. Moreover, the decarbonization policy [1] that has been set by the United Nations in order to reduce global warming has become a turning point for renewable energy in order to generate more clean energy for the future. In this advanced period of smart electrical power systems, the microgrid (MG) technology has shown as one of the promising advances in innovation for the penetration of renewable energy sources (RES) into the existing power grid [2], [3]. The interconnection of small generation systems, such as solar photovoltaic panels, wind generator, and microturbine as well as storage systems, are known as distributed generations (DGs), which connect to the primary network grid through power electronic interference-inverters [4]. The MG based on RES, comprising multiple DGs, local loads, power electronic converters, and energy storage system, has become an alternative electrical network. Meanwhile, advanced technologies together with the current restructuring of wholesale and retail energy markets have opened the possibility for the generation of small energy systems that can give more freedom for users to generate and control the electrical energy in order to meet their own needs [5]. An MG can operate in two different modes [6]; grid operation or autonomous (islanded) operation. The adaptable control of different DGs is necessary to reinforce their reliability and to eliminate the impact of an unstable power supply. Consequently, multilayer hierarchical control architecture is compulsory to accomplish the legitimate operation of the MG due to some reasons.

The multilayer hierarchical control architecture, with a relative intricacy of the MG's operation, is evolving. It comprises three control levels [7]–[10]; 1) the primary control is dedicated to controlling local variables by altering the yield

voltage and frequency of the inverter, which is responsible for good power-sharing, 2) the secondary control fills in as an automatic unified algorithm controller and compensates the steady-state errors in the output voltage and frequency by restoring them to nominal values, and 3) the tertiary control deals with the power exchanged at the point of common coupling (PCC) between the primary network grid and the MG network. Therefore, to accomplish a superior operation of power generation and to improve the reliability of the parallel inverter system, the primary control based on the droop control technique is investigated in this paper.

At the moment, the droop control method is a commonly used technique to control the inverter when connecting multiple DG units in a parallel configuration and to form an islanded MG [11]. The droop technique gives the advantage of eliminating the communication-link mechanism between the inverters as compared to other existing control methods. This approach allows the DGs to execute total power-load demand sharing by adjusting the yield voltage and frequency as elements of the desired active and reactive powers. The inverters can regulate the outputs to ensure accurate power-sharing in light of the relationship between active power and frequency (*P/f*) and reactive power and voltage (*Q/V*) [12] [13]. In the researched current droop control, the operating frequency in the autonomous MG is constantly changed by the variation of load demand, and the frequency restoration process is executed in a more prolonged period [14]. This is because of the slow transient response. As is well known, if the frequency deviation suddenly rises due to load changes and causes the system frequency to deviate more than the rated value of 50 Hz, it will create a power outage to the system. Regardless of the recognized advantages of the droop control, it has a downside of delivering voltage and frequency deviations from the nominal values. In [15], [16] the authors propose an autonomous restoration control to restore the frequency and voltage to their rated values. In addition, the droop controller is unsteady because of the power coupling method and therefore its sharing ends up erroneous. To solve such problems, researchers have improved the traditional droop control. In [17], [18], a virtual impedance is proposed and included in the control circle to make sure the DG output impedance can be inductive. Therefore, it is vital to have an accurate droop controller combined with high-speed frequency tracking in order to generate a precise power-sharing while maintaining the voltage output. Although these improved droop control methods can improve the overall power-sharing accuracy, they have complexities in adjusting the control parameters.

As can be seen from the previous paragraph, there is no comprehensive study of MG in the presence of different power load ratings, but only one kind of load is considered in each study. In addition, there is no study as from the authors' observation of when the DG units connect/disconnect to/from the PCC. Therefore, this paper will explain an initiative for the MG with a change in the primary droop control to analyze the presence of different amounts of rated power to the loads during the DGs' plug-in/out. In this paper, a self-frequency-restoration droop control method is proposed. The proposed control can restore the frequency to a nominal value in a fast manner and an automatic way and with accurately regulated power sharing, where the output power is being controlled by using the coordinate rotation transformation method and being realized as a wholly decoupled relationship between the active and reactive powers. A well-designed frequency restoration unit is introduced where *P/f* is renovated with new characteristics for limiting the frequency deviation due to load changes. The virtual sine active power-frequency droop control is also used. The method makes the frequency restoration to become autonomous to load changes and remain within the allowable limits. The simulation results are given to check and verify the proposed control strategy.

This paper comprises five sections and is arranged as follows. Section II gives an overview of the autonomous MG for the proposed system. Part III introduces the enhancement of the droop control method. The simulation and the results of the analysis are discussed in Section IV. The conclusion of the proposed model is presented in Section V.

2. Islanded Microgrid Configuration

The corresponding proposed structure's configuration for the execution of the controller in a single-phase islanded MG is shown in Fig. 1. The proposed test system comprises a mix of the DG units associated with the local load through the inverter, where every DG unit is related to its respective primary control. The primary point of the proposed control is to track the voltage and frequency of the DGs' output in order to share the active and reactive powers required by the load with faster restoration time.

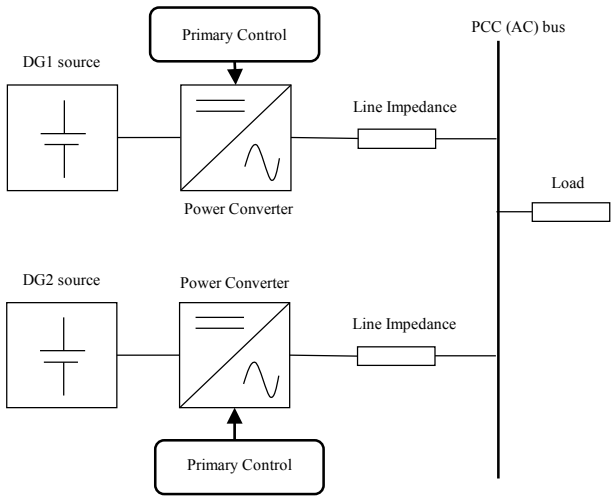

Fig. 1. Block diagram of parallel single-phase DG units connected with primary control.

The primary control, especially in an islanded MG, is based on the droop control technique as depicted in Fig. 5. For this technique, the local power measurement incorporates an inverter with an LCL filter that is controlled by a primary control. A self-droop control loop is used to generate the frequency and voltage of the inverter output as per the ideal reference. Finally, a sine droop reference signal is generated to trigger the pulse-width modulation (PWM) signals for gate-pulse switching purposes.

3. Droop Control Method for the Parallel Single-Phase Connected Inverter

This section explicates the conventional droop control and the implementation of the proposed self-frequency-restoration droop control set for accurate power-sharing with fast frequency restoration. The discussions are categorized into several sub-chapters.

3.1. Review of existing droop control for islanded microgrid

To understand the methodology and origin of the droop control method, consider the issue of complex power transferred by a transmission line. The traditional droop control is reasoned from the supposition of purely inductive line impedance, X [19]. The equivalent per-phase model of an inverter connected to the PCC bus is illustrated in Fig. 2:

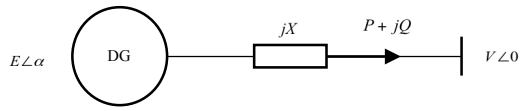

Fig. 2. Equivalent per-phase model of power flow in the transmission line.

where E is voltage of the DG unit, V is voltage at the PCC, $Z=R+jX$ is the comprehensive line impedance from the DG to the PCC, θ is circuit impedance angle, P and Q are active and reactive power flows throughout the line, respectively, and α is output voltage phase angle of the DG unit.

At the point when the inverter's output impedance is absolutely inductive, the inverter per-phase active P and reactive Q powers conveyed into the PCC bus can be expressed as:

$$P = \frac{EV\sin\alpha}{X} \tag{1}$$

$$Q = \frac{EV\cos\alpha - V^2}{X} \tag{2}$$

Based on equations (1) and (2), and with the assumption that the power angle, α is relatively very small (so that sin α ≈ α and cos α = 1) [20], the active power P delivered to the PCC bus is chiefly impacted by α. İn the meantime, the reactive power Q depends on the magnitude difference between the voltages ($E-V$). Thus, simplifying and rewriting the equations gives:

$$\alpha \cong \frac{XP}{EV} \tag{3}$$

$$E - V \cong \frac{XQ}{V} \tag{4}$$

The line impedance is presented to be inductance in a high voltage transmission line, so that X>>R; thus, the resistance can be neglected in the control [21]. The obtained equations in (3) and (4) demonstrate that the power angle depends vigorously on the active power and that the voltage difference relies upon the reactive power. In other words, if the active power can be regulated, so can the power angle at that point, and if the reactive power can be controlled, the voltage E will be controllable at that point also.

However, in the islanded network droop control operation, the units do not know the initial phase values of the units. Therefore, each unit utilizes frequency rather than power or phase angle to control the flow of the active power. Thus, the voltage and frequency can be resolved by controlling the active and reactive power flows through the power system [20], [22]. This prompts the common droop control equations for each inverter:

$$\omega^* = \omega_o - mP \tag{5}$$

$$E^* = E_o - nQ \tag{6}$$

where ω_o and E_o are the nominal frequency and voltage, respectively; P and Q are the measured active and reactive power outputs of the DG unit, respectively; and m and n are the frequency and voltage droop coefficients, respectively. Meanwhile, ω^* and E^* are frequency and voltage measured at the output of the DG unit, respectively.

Fig. 3 shows the droop coefficient characteristic graph. As the active power load on the system increases, the droop technique will permit the frequency and voltage to decrease within the allowable boundary [23]. Meanwhile, Fig. 4 shows the ordinary droop control block diagram. İt comprises three blocks: 1) output voltage and current signal transformation at the fundamental frequency to extract the d–q-components, 2) power calculation to generate the instantaneous active power p and reactive power q, and 3) sine generator to inject the voltage reference to a PWM signal.

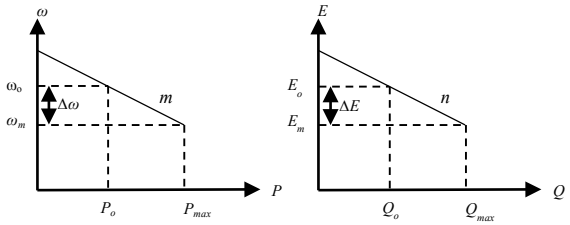

Fig. 3. Droop control characteristic for *P/f* and *Q/V* coefficient.

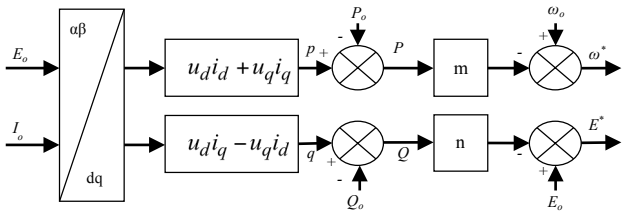

Fig. 4. Block diagram of conventional droop control.

The instantaneous output voltage and current of the inverter are transformed into the rotating reference frame (d–q). Then, the instantaneous active power p and reactive power q are calculated based on the given equation. After that, the reference frequency and voltage of DG units are obtained through the sine droop generator:

$$V_{ref} = E^* \sin\omega^*(t) \tag{7}$$

3.2. The proposed self-frequency-restoration droop control

This technique uses the sine generator droop control to make droop coefficient changes within the rated power. This control strategy can be adjusted automatically to the droop coefficient according to the inverter output power. Naturally, when the output power is unequal, the droop gain is also different. The frequency deviation in the droop method will influence the power-sharing quality. The system frequency is only determined by the DG units. Hence, this paper's concern is on proposing a self-restoration technique in an autonomous operating condition in order to guarantee that the system frequency is in the desirable range.

In a grid network, the frequency deviation as referenced before can be controlled with the secondary frequency loop [24], [25], and this strategy can be implemented in the MG. Generally, in the low-voltage power grid, frequency tolerance is being limited to 50±0.5 Hz. Therefore, a self-frequency-restoration control is presented dependent on a moderate proportional integral (PI) control within the allowable frequency limit.

Fig. 5 shows the suggested block diagram of the self-frequency-restoration droop control by enhancing the *P/f* unit in order to restore the system frequency to the nominal value. As seen, the proposed control strategy uses a PI for the response time assistance in order to generate a fast self-frequency-response. The advantage of having the embedded PI control is due to the ability of the PI control to achieve a faster steady-state time and to reduce the rise time of the measured frequency. Therefore, the measured frequency is compared with the rated value in order to get an error signal, which then is passed through the PI to generate a restoring signal but maintains the frequency. As noticed, the PI parameter values are to have zero steady-state error at the load frequency of 50 Hz without any severe frequency drop during the transient response. Thus, the frequency-restoring signal can be generated in a fast time. As shown in Fig. 6, the two DGs are assumed as the same rated system in terms of power capacity and *P/f* droop coefficient. Notice that the relationship of the frequency droop coefficient and the frequency restoration is controllable by the active power flow in the MG.

Consequently, the restoration is adequate to control the frequency, with the rightfully generated restoring signal f_{sys} and can be expressed as:

$$f_{res} = K_p(f_o - f_{DG}) + K_i(f_o - f_{DG}) \tag{8}$$

where K_p and K_i are the PI parameters, f_o is the rated frequency, and f_{DG} is the measurement frequency. Hence, the self-restoring signal f_{res} is produced to remunerate the deviation on the frequency, where K_p is equal to K_i and is kept constant for control design simplicity. Hence, the improved active power and frequency *P/f* units can be expressed as:

$$f^* = f_o - m_{new}\left(P - P_o\right) \tag{9}$$

$$f^* = f_o - \left[\left(K_p + \frac{K_i}{s}\right)\left(P - P_o\right)\right] \tag{10}$$

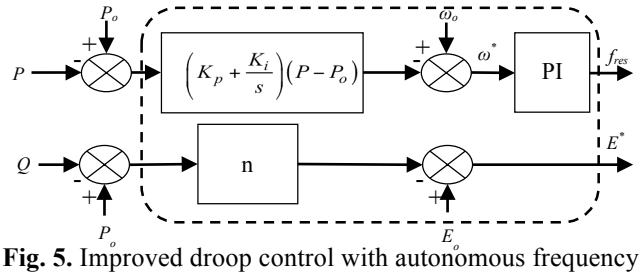

Fig. 5. Improved droop control with autonomous frequency restoration loop.

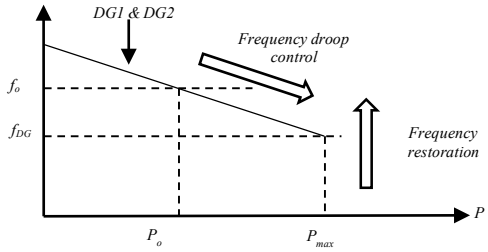

Fig. 6. Frequency droop and restoration curve.

4. Simulation Results

In order to verify the effectiveness of the proposed control, several test cases have been carried out using MATLAB/Simulink that is under load circumstances and DG units in plug-in/out. To observe the active and reactive power dependency on accurate power sharing, a step change in the demand active power is made by the step-response change at 0.1s and 0.3s.

Table 1. Microgrid system parameters

Parameters	Units	Value
L_f	*H*	3×10^{-3}
C_f	*F*	52×10^{-6}
L_g	*H*	1×10^{-3}
V_{dc}	*V*	400
V_n	*V*	230
F_o	*Hz*	50
m	*rad/(W.s)*	0.05
n	*V/Var*	0.03
K_p	*rad/s*	1.798
K_i	*rad/s-*	838

The autonomous MG in Fig. 7 illustrates the DGs' test system. It consists of two DG units that have identical parameters and is associated with the external loads L_1 and L_2 with different power load ratings. This local load is connected to the system in bus-connected and will be activated by the step responses S_1 and S_2. Table 2 presents the load value change in Case 1 and Table 3 presents the load when the DG units are in plug-in/out in Case 2.

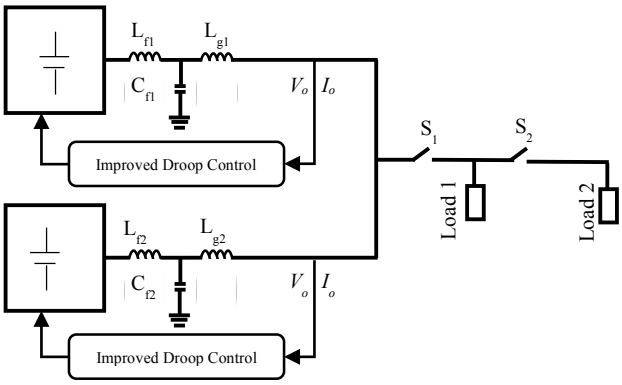

Fig. 7. Diagram of parallel DGs associate with the load.

Table 2. Load and power rating for load change

Variable	Unit	Power Rating	ON time
Load 1	P_{L1}, W	1500	0.1s
	Q_{L1}, VAR	113	
Load 1	P_{L2}, W	3000	0.3s
	Q_{L2}, VAR	226	

Table 3. Inverter load and power rating with connection time

Inverter	Power Rating	ON time	OFF time
DG1	P_{L1}= 500W	0s	-
DG2	P_{L2}=750W	0.1s	0.3s

4.1. Performance of improved droop control response

Fig. 8 shows the time evolution of transient response for the reference value set-point. As noticed, the set-point for the reference value should be set at 50 Hz, and the controller instantly responded to track the desired rated frequency. The rise time for the controller to follow the reference signal is 0.028s. Since the desired gain values are kept the same, similar conditions occur for the voltage set-point.

The tabulated comparison data between the conventional and the proposed controllers is presented in Table 4. The time evolution for transient response is indicated in a fast period at 0.0042s, whereas the traditional controller records a slower period at 0.0077s. The transient time response of the improved droop control is 0.0035s faster than the previous method. It shows that the correlation between frequency restoration and PI can ensure a stable system frequency and voltage at nominal values.

Table 4. Comparison summary for transient time response

Parameter	Conventional	Proposed
Transient time response (s)	0.0077	0.0042
Steady-state time (s)	0.0200	0.0100
Rise time (s)	0.0085	0.0028

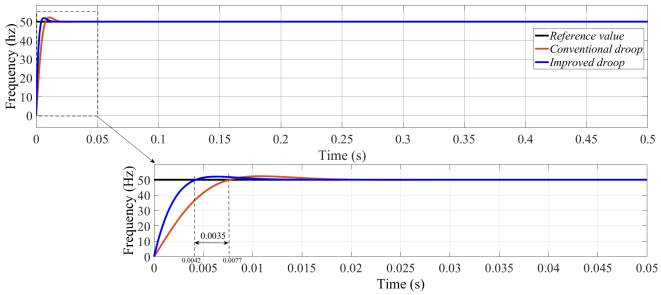

Fig. 8. Transient time response at set-point frequency 50 Hz.

4.2. Case 1: Load change assessment

The test for Case 1 is completed with a difference in load value by including an external load at 0.1s and 0.3s. Both DG1 and DG2 are assumed to have the same parameters. Fig. 6 depicts the time evolution of the active and reactive powers, output voltage, and load current consumptions of DG1 and DG2. Since both DG units have identical parameters, the active and reactive powers are different from each other. As seen in Fig. 9(a), the inverter individually pushes 600 W active power to the PCC as load required. At 0.1s, when L_1 is connected to the system, the inverter instantly transfers 620 W active power per load demand. At t=0.3s, L_2 is connected, and the active power is boosted up to 1345 W and pushed to the PCC. The total reactive power transfer is shown in Fig. 9(b) with the measured values of 38 VAR and 124 VAR. Figs. 9(c)–(d) show the inverter voltage output and the donated total load current of 325 V and 8.6 A, respectively. As noticed, all loads consume the average current according to power load capacities. It indicates that the inverters regulate load current in a smooth transient procedure when load circumstances are actuated.

The improved droop control is focused on accurate power sharing among the DGs while keeping the system frequency at a nominal value. The powers are transferred instantaneously and autonomously. It validates that the power-sharing accuracy is guaranteed with the help of frequency restoration.

4.3. Case 2: DG units in plug-in/out

The objective of this simulation study is to test and verify the power-sharing capability embedded with the self-frequency-restoration droop control in an islanded bus-connected MG. With the help of the proposed control, the DG units have the ability to handle the 'on and off' operation of the MG. To achieve this objective, DG1 begins to supply the load at 0.1s, and then DG2 is connected and disconnected to/from the microgrid at 0.1s and 0.3s, respectively. As illustrated in Fig. 10(a)–(b), at the point when the DG2 is connected, the active and reactive powers of DG1 and DG2 are equally shared at 313 W and 1.7 VAR, respectively, which implies that the powers conveyed to the load are shared between those DGs. Meanwhile, Figs. 10(c)–(d) show the microgrid's voltage and total load current consumption when the system receives an external DG. As seen from 0.1s to 0.3s, the current is shared equally among the DGs at 2 A. After 0.3s, the controller transient smoothly reverts the load current to the nominal value as per required.

Meanwhile, Fig. 11 shows the summary results for the system frequency under the proposed controller as compared to the conventional droop control. The results show that the proposed control strategy is able to restore the frequency in a faster time when compared to the conventional method, which takes a prolonged time as can been seen at time 0.25s in Figs. 9(a)–(b). The frequency magnitude for the proposed method is 49.87 Hz while the frequency magnitude for the existing method is 49.78 Hz, which indicated that the proposed method is able to reduce the frequency deviation when the active power changes. Notice that the proposed control restores frequency in a fast manner with fast transient tracking of within 0.0035s as compared to conventional droop, which is lagging at within 0.0077s.

The presented summary results prove that with proper desired control gain, the power is instantly transferred once the controller is activated, while the system frequency is autonomously restored to a nominal value. It validates that the controller response reacts immediately to restore the system frequency, thus ensuring accurate power sharing among the DGs. The controller can instantly transfer the required power load and current according to load capacities with minimum time. The effectiveness of the proposed power control in an autonomous microgrid is demonstrated from the presented results, making it appropriate to be applied in a single-phase low-voltage network.

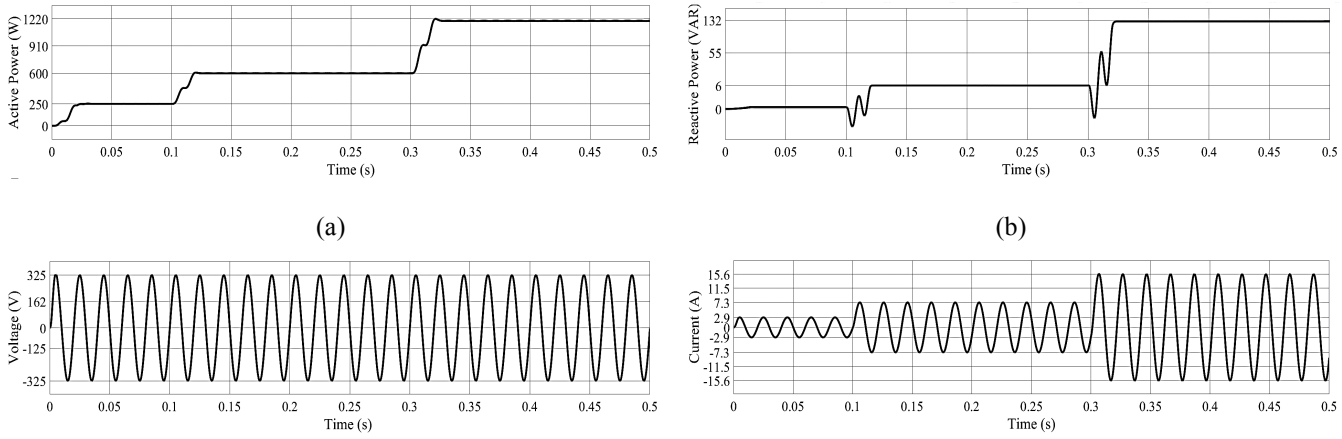

Fig. 9. Simulated results of Case 1: (a) load active power, (b) reactive power, (c) system output voltage, and (d) load current consumptions.

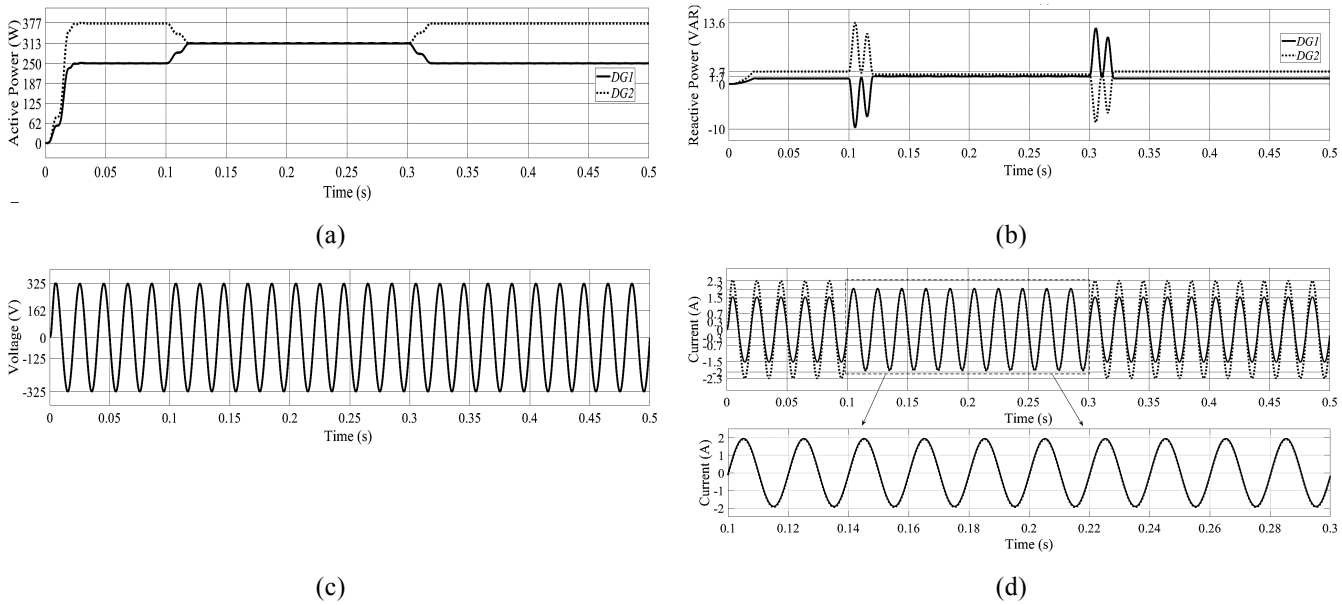

Fig. 10. Simulated results of Case 2: (a) load active power, (b) reactive power, (c) system output voltage, and (d) load current consumptions.

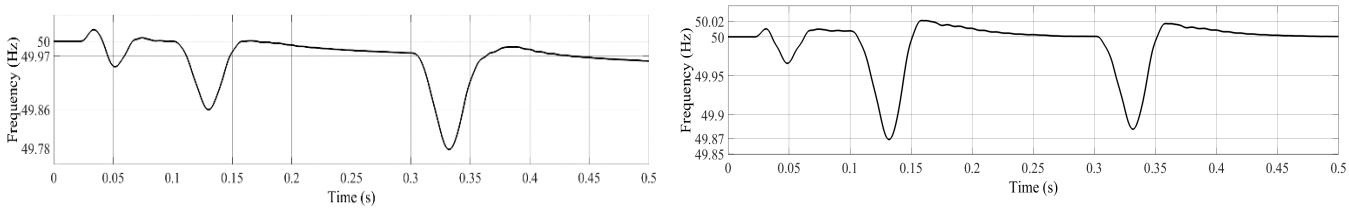

Fig. 11. System frequency restoration: (a) conventional droop control, (b) proposed self-frequency-restoration droop control.

4.4. Comparative analysis of proposed droop control with conventional droop control

Fig. 12 shows the time evolution of the operating frequency of the MG under the proposed self-frequency-restoration droop technique as compared to the traditional droop control. As noticed, when load change occurs, the new restoration control is able to regulate the inverter's output frequency while restoring it to the nominal value regardless of the amount of power load changes. Consequently, the system's output voltage and frequency are drooped to new nominal values to guarantee that load sharing can be directed. As shown in the obtained results, it is noticed that the self-frequency-restoration droop control can restore the operating frequency in a faster time and seamlessly as well. It shows that the proposed controller has a higher capability for frequency restoration at 50 Hz compared to the conventional droop control under changing load conditions.

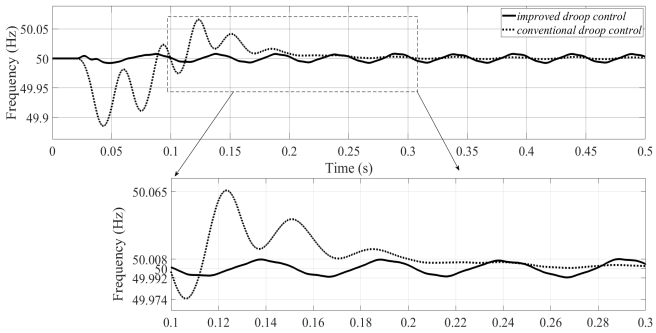

Fig. 12: System frequency restoration for proposed improved droop control as compared to conventional droop control.

5. Conclusion

As a conclusion, this paper proves that a frequency self-restoration embedded with the droop control method increases the frequency stability in maintaining the allowable rated frequency and also responding for an accurate power-sharing during load changes that happen in an islanded microgrid. The performance of the proposed controller is verified with several tests thoroughly regarding power sharing as well as frequency and voltage regulation at the converter side. Combined with the PI control technique that is embedded together within the restoration loop, it provides a fast voltage-frequency tracking with minimal initial transient response time and better steady-state performance. Simulation results show the feasibility and effectiveness of the proposed control strategy. It is able to adjust and keep the voltage and frequency at nominal values in order to provide smooth load demand regarding active and reactive power demand. Furthermore, the frequency deviation during load change is also minimized to the limit of the allowable frequency. The smooth frequency restoration is to ensure that the microgrid will not be burdened by the overstressing of the load in order to avoid high dynamic swing to the microgrid. In summary, the proposed controller will create an autonomous microgrid system whereby the DGs are able to operate as an independent control system.

Acknowledgments

This work is supported and financed by the Research University Grant Programme in UTHM under Vot number U998. The UTHM Centre for Graduate Studies and Research Management Centre fund for partly sponsors this paper. In addition, the authors would like to thank the Advanced Control in Power Converter Team for the research work conducted.

References

[1] B. S. Abdulraheem and C. K. Gan, "Power system frequency stability and control: Survey," *International Journal of Applied Engineering Research*, vol. 11, no. 8, pp. 5688–5695, 2016.

[2] D. E. Olivares *et al.*, "Trends in microgrid control," *IEEE Transactions on Smart Grid*, vol. 5, no. 4, pp. 1905–1919, 2014.

[3] P. Mazidi, G. Baltas, and M. Eliassi, "A Model for Flexibility Analysis of RESS with Electric Energy Storage and Reserve," *7th International Conference on Renewable Energy Research and Applications*, vol. 5, pp. 1–6, 2017.

[4] J. Song, S. J. Song, S. D. Oh, and Y. Yoo, "Optimal Operational State Scheduling of Wind Turbines for Lower Battery Capacity in Renewable Power Systems in Islands," *5th International Conference on Renewable Energy Research and Applications*, vol. 5, pp. 5–9, 2016.

[5] J. A. Mueller and J. W. Kimball, "An Efficient Method of Determining Operating Points of Droop-Controlled Microgrids," *Transaction on Energy Conversion*, vol. 8969, pp. 1–15, 2017.

[6] K. S. Rajesh, S. S. Dash, R. Rajagopal, and R. Sridhar, "A review on control of ac microgrid," *Renewable and Sustainable Energy Reviews*, vol. 71, no. 1, pp. 814–819, 2017.

[7] R. Palma-Behnke *et al.*, "A Microgrid Energy Management System Based on the Rolling Horizon

Strategy," *IEEE Transactions on Smart Grid*, vol. 4, no. 2, pp. 996–1006, 2013.

[8] I. Azim, "An Inverter Control Technique for an RES-based Islanded Microgrid," *International Journal of Renewable Energy Research*, vol. 6, no. 2, pp. 581–584, 2016.

[9] M. T. Tsai, L. C. Chu, and W. C. Chen, "Implementation of a serial AC/DC converter with modular control technology," *7th International Conference on Renewable Energy Research and Applications*, vol. 5, pp. 3–8, 2018.

[10] S. Heo, W. K. Park, and I. Lee, "Single-phase Power Conditioning System with Slew-Rate Controlled Synchronizer for Renewable Energy System in Microgrid," *5th International Conference on Renewable Energy Research and Applications*, vol. 5, pp. 3–8, 2016.

[11] U. B. Tayab, M. A. Bin Roslan, L. J. Hwai, and M. Kashif, "A review of droop control techniques for microgrid," *Renewable and Sustainable Energy Reviews*, vol. 76, no. May 2016, pp. 717–727, 2017.

[12] A. Vinayagam, K. S. V. Swarna, S. Y. Khoo, A. T. Oo, and A. Stojcevski, "PV Based Microgrid with Grid-Support Grid-Forming Inverter Control-(Simulation and Analysis)," *Smart Grid and Renewable Energy*, vol. 8, no. 1, pp. 1–30, 2017.

[13] L. Meng *et al.*, "Review on Control of DC Microgrids and Multiple Microgrid Clusters," *IEEE Journal of Emerging and Selected Topics in Power Electronics*, vol. 5, no. 3, pp. 928–948, 2017.

[14] C. R. Reddy and K. Harinadha Reddy, "Islanding detection for inverter based distributed generation with Low frequency current harmonic injection through Q controller and ROCOF analysis," *Journal of Electrical Systems*, vol. 14, no. 2, pp. 179–191, 2018.

[15] P. H. Divshali, A. Alimardani, S. H. Hosseinian, and M. Abedi, "Decentralized Cooperative Control Strategy of Microsources for Stabilizing Autonomous VSC-Based Microgrids," *IEEE Transactions on Power Systems*, vol. 27, no. 4, pp. 1949–1959, 2012.

[16] A. Khaledian and M. A. Golkar, "Analysis of droop control method in an autonomous microgrid," *Journal of Applied Research and Technology*, vol. 15, no. 4, pp. 371–377, 2017.

[17] W. Yao, M. Chen, J. Matas, J. M. Guerrero, and Z. M. Qian, "Design and analysis of the droop control method for parallel inverters considering the impact of the complex impedance on the power sharing," *IEEE Transactions on Industrial Electronics*, vol. 58, no. 2, pp. 576–588, 2011.

[18] J. Simpson-Porco, Q. Shafiee, F. Dörfler, J. C. Vasquez, J. M. Guerrero, and F. Bullo, "Secondary Frequency and Voltage Control of Islanded Microgrids via Distributed Averaging Secondary Frequency and Voltage Control of Islanded Microgrids via Distributed Averaging," *IEEE Transactions on Industry Electronics*, vol. 62, no. April 2016, pp. 7025–7038, 2015.

[19] J. He and Y. W. Li, "An enhanced microgrid load demand sharing strategy," *IEEE Transactions on Power Electronics*, vol. 27, no. 9, pp. 3984–3995, 2012.

[20] R. Jackson, S. A. Zulkifli, N. Mazliza, and B. Sham, "Power Flow Control Scheme for Hybrid Single-Phase Energy System Using Droop Control : a Comprehensive Survey," *International Review of Electrical Engineering*, vol. 13, no. 8, pp. 305–315, 2018.

[21] T. H. Nguyen, K. Al Hosani, N. Al Sayari, and A. R. Beig, "Seamless transition scheme between grid-tied and stand-alone modes of distributed generation inverters," *2017 IEEE 3rd International Future Energy Electronics Conference and ECCE Asia, IFEEC - ECCE Asia 2017*, pp. 344–349, 2017.

[22] N. Sakib, J. Hossain, H. I. Bulbul, E. Hossain, and R. Bayindir, "Implementation of Unit Commitment Algorithm: A Comprehensive Droop Control Technique to Retain Microgrid Stability," *5th International Conference on Renewable Energy Research and Applications*, vol. 5, pp. 1074–1079, 2016.

[23] P. Stumpf, I. Nagy, and I. Vajk, "Novel Approach of Microgrid Control," *3rd International Conference on Renewable Energy Research and Applications*, pp. 859–864, 2014.

[24] S. Ahn, J. Choi, S. Ahn, and J. Choi, "Power Sharing and Frequency Control of an Autonomous Microgrid Considering the Dynamic Characteristics of Distributed Generations Power Sharing and Frequency Control of an Autonomous Microgrid Considering the Dynamic Characteristics of Distributed Generat," *Journal of International Council on Electrical Engineering*, vol. 2, no. 1, pp. 39–44, 2014.

[25] W. Cao, H. Su, J. Cao, J. Sun, and D. Yang, "Improved Droop Control Method in Microgrid and Its Small Signal Stability Analysis," *3rd International Conference on Renewable Energy Research and Applications*, pp. 197–202, 2014.